

SIMULATION STUDY ON BUNCH COMPRESSION AND DECOMPRESSION FOR GENERATION OF COHERENT THZ RADIATION AT THE COMPACT ERL *

N. Nakamura, M. Shimada, T. Miyajima, K. Harada, O. A. Tanaka, A. Ueda,
High Energy Accelerator Research Organization (KEK), Tsukuba, Ibaraki, Japan

Abstract

We study bunch compression and decompression in the Compact Energy Recovery Linac (cERL) at KEK by using simulations to achieve an ultra-short bunch for generation of the THz coherent radiation planned for the near future. In this study, off-crest acceleration in the main superconducting linac and non-zero R_{56} optics in the two arc sections are used and sextupole magnets are introduced into the two arc sections for optimizing T_{566} of the arc sections. The results of the simulation study show that the bunch can be compressed to less than 50 fs and then almost decompressed to the initial bunch length.

INTRODUCTION

The commissioning of the entire cERL was started in December 2013 and the beam recirculation and energy recovery were achieved in February 2014[1]. In 2015, the maximum average current was recorded at about 80 μ A and laser-Compton scattering X-rays was successfully generated[2]. In the next step, generation of THz coherent radiation is planned for the near future.

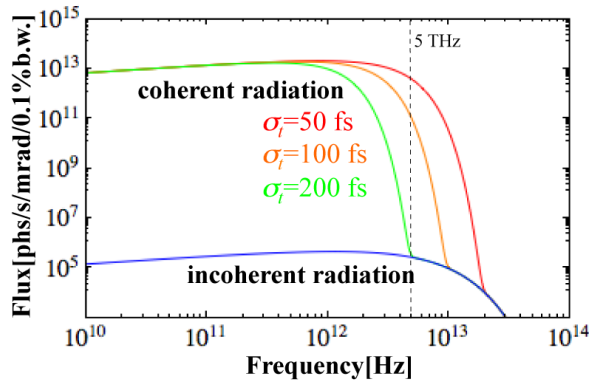


Figure 1: CSR spectra of the 20 MeV cERL for three different bunch lengths of 50, 100 and 200 fs, at the bunch charge of 7.7 pC and the bunch repetition frequency of 130 kHz.

The coherent synchrotron radiation (CSR) spectra generated at a bending magnet of the arc sections are calculated and shown in Fig. 1. An electron bunch less than 100 fs is required for providing intense THz-CSR up to 5 THz to users. We simulate bunch compression and decompression in the cERL by using a tracking code ELEGANT [3] to check the feasibility of generating such

*norio.nakamura@kek.jp

an ultra-short bunch. In the bunch compression and decompression simulation, sextupole magnets were added in the two arc sections for optimizing T_{566} of the arc sections. In this paper, we present the simulation results and requirements for the sextupole magnets including their field strengths, number and layout.

LINEAR OPTICS AND SEXTUPOLE MAGNETS OF ARC SECTIONS

Linear Optics

In the bunch compression and decompression scheme of the cERL, the bunch is accelerated off-crest in the main superconducting linac to have a correlation between the energy and longitudinal position and then the bunch length is compressed in the 1st arc section with a positive R_{56} value. After the bunch compression, the bunch length is decompressed through the 2nd arc section with a negative R_{56} value and then decelerated off-crest to compress the energy spread to the initial value before the beam enters the dump line. Figure 2 shows the linear optics of the arc section with three different R_{56} values. The optics with $R_{56}=0$ is used in the normal operation and the optics with $R_{56}=0.15$ m and $R_{56}=-0.06$ m correspond to the 1st and 2nd arc sections in the bunch compression and decompression operation, respectively.

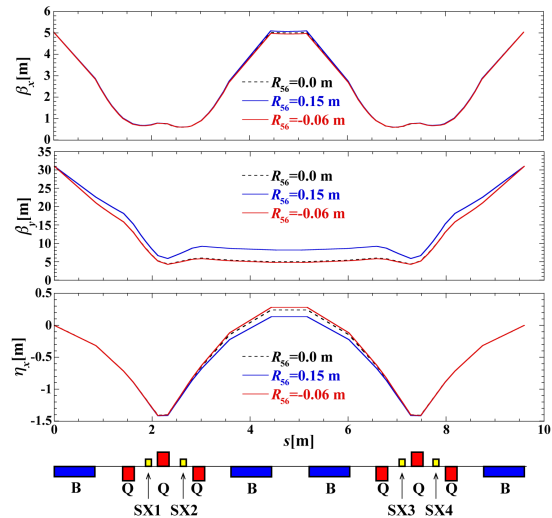


Figure 2: Horizontal and vertical betatron functions (β_x , β_y) and dispersion function (η_x) of the arc sections with three different R_{56} values of 0.0 m (black broken line), 0.15 m (blue solid line) and -0.06 m (red solid line). B, Q and SX1-4 indicate the bending, quadrupole and sextupole magnets, respectively.

Sextupole Magnets

Sextupole magnets must be introduced in the two arc sections for the second-order correction of the energy-dependent path length (T_{566} correction). In each arc section, all or any of four sextupole magnets from SX1 to SX4 with the length of 10 cm can be inserted for the bunch compression and decompression as shown in Fig. 2. In order to decide the required number and field strengths and the optimum layout of the sextupole magnets for the 1st arc section, the bunch compression simulation is first performed. Here the beam energies at the entrance and exit of the main linac are 2.9 MeV and 20 MeV. We set the bunch charge to 7.7 pC and assume the initial bunch distribution at the entrance of the main linac to be a six-dimensional Gaussian distribution with the bunch length of 2 ps, the relative momentum spread of 0.1 % and the horizontal and vertical normalized emittances of 1 mm·mrad. In this bunch compression simulation, the bunch length is minimized at the exit of the 1st arc section by optimizing the main-linac RF phase and sextupole magnet strengths.

Table 1: Simulation Result of Bunch Compression

Sextupole magnets	σ_t^* [fs]	$\epsilon_{nx}/\epsilon_{ny}^\#$ [mm·mrad]	K_2^\dagger [m ⁻²]
SX1-4 OFF	875	1.14/1.03	-
SX1-4 ON	60.6	1.13/1.16	-14.9, -33.3 -21.0, -22.2
SX1 ON	65.7	1.60/1.35	-106.4
SX2 ON	66.4	1.59/1.16	-84.6
SX3 ON	74.4	1.95/1.20	-112.2
SX4 ON	67.4	1.55/1.19	-80.2
SX1&2 ON	65.3	1.50/1.26	-62.4, -34.7
SX1&3 ON	61.4	1.18/1.25	-69.8, -38.8
SX1&4 ON	62.6	1.32/1.23	-69.4, -28.2
SX2&3 ON	62.2	1.27/1.15	-60.6, -31.5
SX2&4 ON	60.9	1.13/1.15	-42.4, -40.1
SX3&4 ON	68.5	1.65/1.19	-54.3, -41.0

*. # Bunch length and hor./vert. normalized emittances at the exit of 1st arc † Strengths of sextupole magnets of the 1st arc

Table 1 shows the bunch length and the horizontal and vertical normalized emittances at the exit of the 1st arc section and the required sextupole magnet strengths obtained from the bunch compression simulation. Figure 3 shows the change of time-momentum distribution in the bunch compression process for SX2&4 ON and SX1-4 OFF listed in Table 1. The bunch length is effectively reduced from 875 fs to less than 100 fs by excitation and optimization of the sextupole magnets. Combination of SX2 and SX4 (SX2&4 ON) has almost the same performance in bunch compression as all of SX1-4 (SX1-4 ON). For this combination, the emittances are well

preserved probably because the betatron phase advance between the two magnets is the nearest to 90 degrees. In addition, T_{166} and T_{266} of the 1st arc section are also comparatively small. Therefore we decide to choose the combination of SX2 and SX4 for the arc sections.

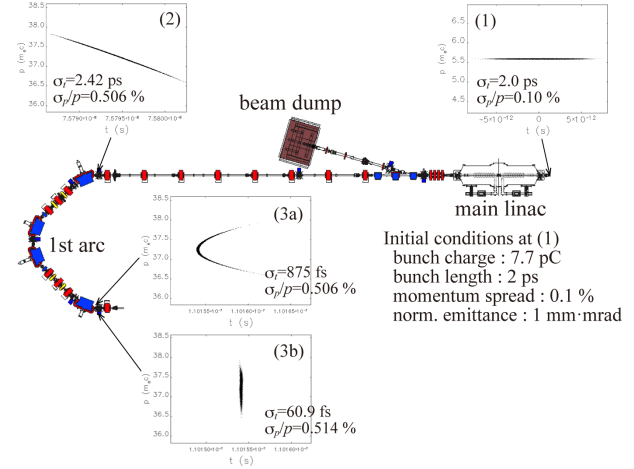


Figure 3: Change of time-momentum (t, p) distribution of the electron bunch from before the main linac to after the 1st arc section in the bunch compression process. The numbers on the distribution plots mean their temporal order. (3a) and (3b) correspond to two cases of SX1-4 OFF and SX2&4 ON listed in Table 1. The bunch length and momentum spread are also shown on each plot. In the simulation, the bunch length is minimized at the exit of the 1st arc section.

BUNCH COMPRESSION AND DECOMPRESSION SIMULATION

In this section, both bunch compression and decompression are simulated. Similarly we assume the initial bunch distribution at the entrance of the main linac to be a six-dimensional Gaussian distribution with the bunch charge of 7.7 pC, the bunch length of 1 or 2 ps, the relative momentum spread of 0.1 % and the horizontal and vertical normalized emittances of 1 mm·mrad. The bunch length is minimized at the entrance of the 2nd arc section, which is very close to the planned THz-CSR port at the 1st bending magnet of the 2nd arc section. Then the bunch is decompressed through the 2nd arc and the momentum spread is minimized at the entrance of the dump line by optimizing the sextupole magnet strengths of the 2nd arc and the decelerating RF phase of the main linac in order to recover the initial bunch state.

The present beam energy of the cERL (20 MeV) is sufficiently low so that the momentum or velocity difference of electrons in the bunch gives the significant difference of the arrival time or effective difference of path length R_{56}^{eff} , which is expressed with the Lorentz factor γ and the velocity normalized by the speed of light β as follows:

$$R_{56}^{\text{eff}} = -\frac{L}{\gamma^2 \beta} \quad (1)$$

Here L is the path length. The effective difference of the path length due to the momentum difference is negative. Furthermore the bunch passes the three chicanes with negative R_{56} values of -0.0101 m, -0.0059 m and -0.0032 m from the exit of the 1st arc to the entrance of the dump line. Therefore we set the R_{56} values of the 1st and 2nd arc sections to 0.15 m and -0.06 m. Their absolute R_{56} values are not equal because of effects of the R_{56}^{eff} and the chicanes. The two optics with R_{56} =0.015 m and -0.06 m are shown by blue and red solid lines in Fig. 2.

Table 2: Simulation Result of Bunch Compression and Decompression

Sextupole magnets	σ_t^* [fs]	$\sigma_p/p^\#$ [%]	K_2^\dagger [m ⁻²]
SX2&4 ON	45.2	0.384	-52.3, -35.0
($\sigma_{t0}^\ddagger=1$ ps)	1195	0.115	-64.4, -40.8
SX2 ON	50.1	0.390	-89.8
($\sigma_{t0}=1$ ps)	1287	0.103	-109.7
SX2&4 ON	45.3	0.777	-52.2, -35.1
($\sigma_{t0}=2$ ps)	2387	0.114	-56.6, -46.3
SX2 ON	69.4	0.779	-89.8
($\sigma_{t0}=2$ ps)	2648	0.383	-116.5

*. # Bunch length and momentum spread at the entrance of 2nd arc after bunch compression (upper row) and at the entrance of the dump line after bunch decompression (lower row) [†] Strengths of sextupole magnets of the 1st arc (upper row) and of the 2nd arc (lower row) [‡] Initial bunch length at the entrance of the main linac

Table 2 shows the simulation result of the bunch compression and decompression at the cERL. Figure 4 shows change of the time-momentum (t, p) distribution of the electron bunch along the cERL for the initial bunch length of 1 ps and SX2&4 ON. When the sextupole magnets of SX2 and SX4 are used in the both arc sections for the simulation, the bunch is compressed to about 45 fs for the two initial bunch lengths of 1 and 2 ps and almost recovered to the initial bunch state in both bunch length and momentum spread. On the other hand, when only SX2 is used, the bunch decompression fails for the initial bunch length of 2ps.

CONCLUSIONS

The bunch compression and decompression simulations demonstrate that the bunch can be compressed down to less than 50 fs and then almost decompressed to the initial bunch length. From the simulation results, we select the combination of two sextupole magnets SX2 and SX4 for each arc section. Four sextupole magnets are being fabricated and will be installed in 2015 to produce an ultra-short bunch for generating THz coherent radiation.

REFERENCES

- [1] N. Nakamura et al., Proc. of IPAC'14, Dresden, Germany, p.353 (2014).
- [2] R. Takai et al., FROM03, in these proceedings.
- [3] http://www.aps.anl.gov/Accelerator_Systems_Division/Accelerator_Operations_Physics/manuals/elegant_t_latest/elegant.pdf

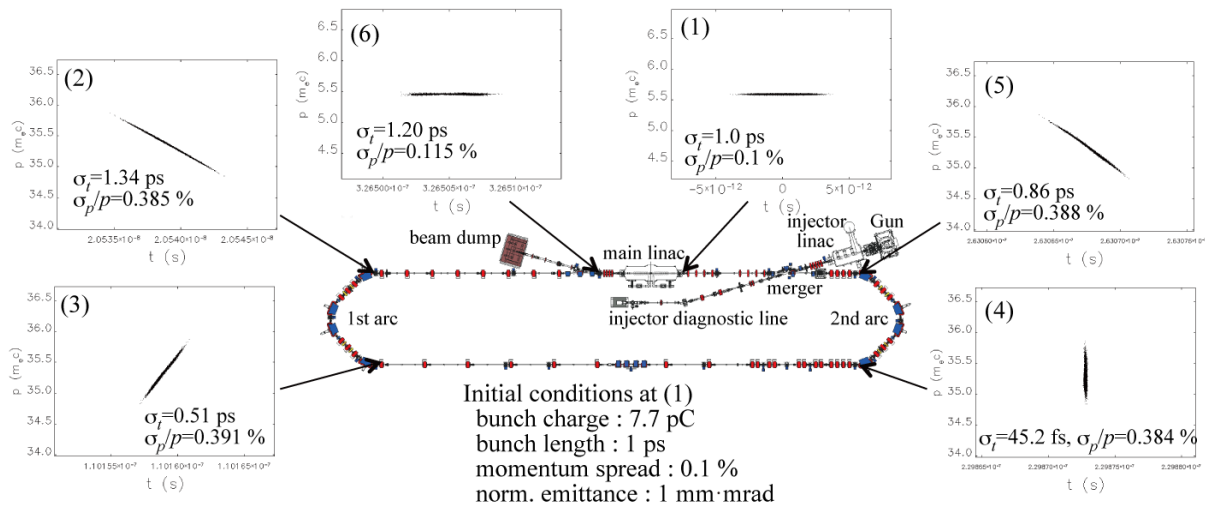


Figure 4: Change of time-momentum (t, p) distribution of the electron bunch along the cERL when SX2 and SX4 are used. The numbers on the distribution plots mean their temporal order. The bunch length and momentum spread are also shown on each plot. In the simulation, the bunch length is minimized at the entrance of the 2nd arc section (4) and the momentum spread at the entrance of the dump line (6).